

RHEOLOGICAL PROPERTIES OF HEAVY CRUDE OIL CONTAINING SAND FROM BO-HAI OILFIELD IN CHINA

DONG ZHANG^{1,2}, SHUO LIU^{1,2}, JIAN ZHANG¹, AND JING-YU XU^{1,2*}

¹Institute of Mechanics, Chinese Academy of Sciences, Beijing 100190, China

²School of Engineering Sciences, University of Chinese Academy of Sciences, Beijing 100049, China

*Corresponding author: xujingyu@imech.ac.cn

Received: 7.9.2016, Final version: 11.1.2017

ABSTRACT:

This paper presents an experimental study on the rheological properties of heavy crude oil containing sand to determine the effects of sand size distribution and mass concentration on apparent viscosity, thixotropic behavior, yield stress and viscoelastic properties. The results of these analyses demonstrate that heavy crude oil containing sand shows strong shear-thinning behavior and a certain degree of thixotropic properties. After blending heavy crude oil with sand, the apparent viscosity and the area of the thixotropic loop first decrease and then steadily increase with increasing sand mass concentration. At a fixed mass concentration, apparent viscosity appears to increase with increasing particle size, while yield stress decreases. Moreover, adding sand generally enhances the elastic modulus of heavy crude oil, while the complex viscosity remains slightly less than the apparent viscosity. These results provide new information helpful for removing sand from heavy crude oil.

KEY WORDS:

Heavy crude oil, sand, viscosity, thixotropy, yield stress, viscoelasticity

1 INTRODUCTION

Heavy crude oil is defined as any liquid petroleum with an API gravity of less than 20°. Crude oil with 10 API or less is considered to be extra heavy oil or bitumen, which is denser than water [1]. Heavy crude oil is a vitally important component of the world's recoverable oil reserves. However, it is extremely difficult to transport heavy crude oil, due to its high viscosity and complex rheological behavior [2, 3]. Current rheological studies of heavy crude oil have primarily focused on factors such as yield stress, thixotropy, and viscoelasticity [4–12]. In studying the yielding behavior of waxy crude oil, Soares et al. [9] concluded that waxy crude oils can be classified as apparent yield stress fluids, and not true yield stress materials, within the presence of a dynamic and a static yield stress. Mortazavi-manesh and Shaw [10] investigated the thixotropic rheological behavior of Maya crude oil: Their results demonstrated that the magnitude of the thixotropic effect is larger at lower temperatures and that stress growth, which occurs as a result of a step-down in the shear rate, is correlated with temperature. The viscoelastic properties of heavy oil and bitumen are mainly related to their composition and temperature [11]. With decreasing temperature, wax crystals and colloidal asphaltene particles can lead to obvious non-Newtonian characteristics [12].

In practice, during its output, heavy crude oil produced from wellheads usually entrains sand, clay, or other porous solids. Therefore, this heavy crude oil containing sediment grains exhibits more complex rheological properties than does regular crude oil. In recent decades, much research has focused on better understanding the rheological properties of these suspensions. Generally, the rheological properties of suspensions can be affected by parameters such as those of the solid fraction, particle sizes and size distributions, and the viscosity of the suspending liquid [13]. Oil sands are an important component of unconventional petroleum resources due to their abundant reserves and their use in the commercial production of bitumen. However, it is essential to liberate heavy crude oil from its host rocks. Dai and Chung [14] revealed that particle size is a critical factor affecting the liberation of bitumen from sand: Namely, the finer the particles, the stronger the attachment. Hasan et al. [15] investigated the rheological properties of Maya crude oil containing solid maltenes and concluded that solid maltenes play a crucial role in determining the rheological properties of heavy oil. By measuring the yielding behavior of oil sand slurries, Gutierrez and Pawlik [16] concluded that the yield values of oil sand slurries increase with increasing bitumen contents in ores. Furthermore, Koenigsberg and Selverian [17] demonstrated that ex-

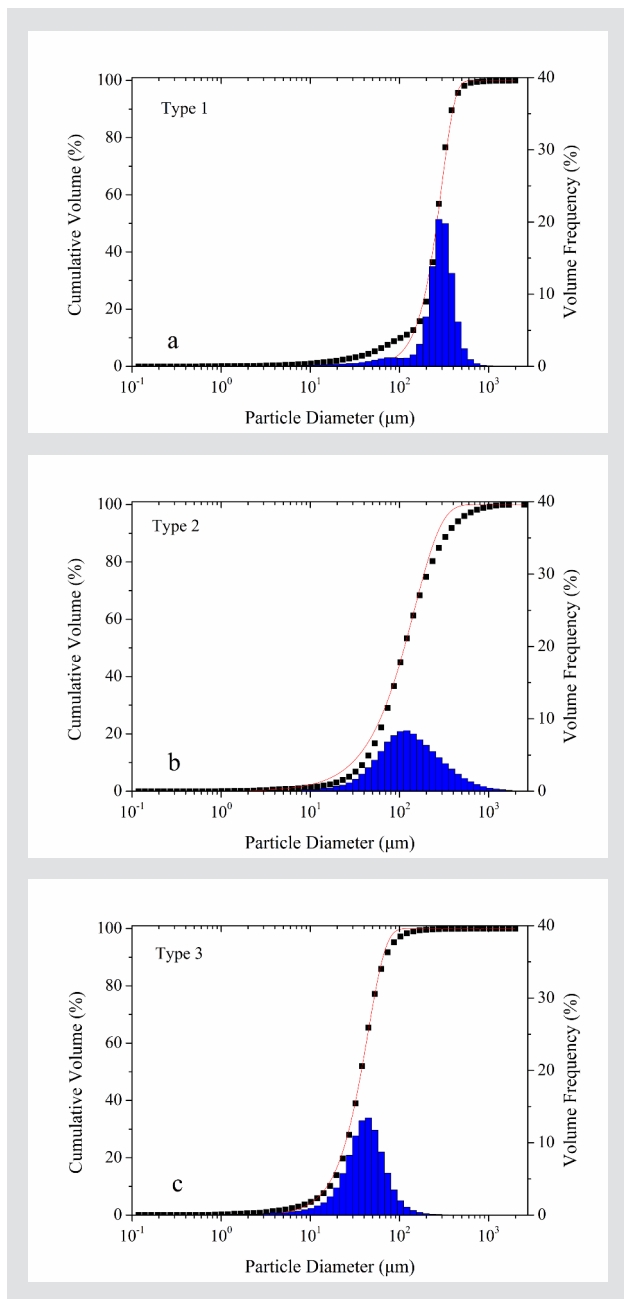


Figure 1: Sand size distributions of the three types.

ponential integral functions can better fit experimental data than can the traditional Prony series for relaxation data obtained from tensile loading of an asphalt-sand mixture. In cases of heavy oil and water emulsions containing sand, Jamaluddin et al. [18] demonstrated that emulsions containing the polymer improved sand-retention characteristics and that the water-wet characteristic of the produced sand enhanced sand dropout.

		Density, ρ_s (kg/m^3)	SARA analysis (wt %)
Heavy crude oil	955		Saturates 33.2
			Aromatics 26.2
			Resins 37.2
			Asphaltenes 3.4

Table 1: Several basic properties of heavy crude oil.

However, the presence of sand at a concentration of 0.05 (v/v) had a minor effect on the oil viscosity. A similar phenomenon was also observed in the work of Yaghi [19]. Although numerous studies have been undertaken to better understand the process of bitumen liberation from oil sands, such as the water-based extraction process applied to Canadian oil sands, the current understanding of the rheological properties of heavy crude oil containing sand remains rather limited. Therefore, this study focuses on constraining the rheological properties of heavy crude oil containing sand from the Bo-hai oilfield in China.

2 MATERIALS AND EXPERIMENTS

2.1 MATERIALS

The heavy crude oil studied in this work comes from the Bo-hai oilfield in China. Several basic properties of this oil are listed in Table 1. Sand samples were obtained from riverbeds and had a mass water content of 12.7%. To achieve the desired sediment mass concentration, a dryer was used to dry these sand samples. Sand grain sizes and their size distributions were measured using a Malvern INSITEX SX Laser Particle Size Analyzer. Three different types of sand size distributions were used to study the effects of sand size distribution on the rheological properties of the heavy crude oil with basic properties of these sands are summarized in Table 2. Heavy crude oil samples can be placed into one of three categories, based on the sand size distributions blended within the oil: crude oil containing type 1 sediment is defined as sample 1, crude oil containing type 2 sediment is defined as sample 2, and crude oil containing type 3 sediment is defined as sample 3. Here, sample 2 is used to study the effects of sand mass concentration on the rheology of the mixture. Heavy crude oil was blended with sand in five different mass concentrations of 0.05, 0.1, 0.15, 0.2, and 0.25 g/mL. Figure 1 depicts the sand size distributions of these three types. The cumulative volume is displayed as an S-type curve, which can be described using the Rosin-Rammler distribution function. This Rosin-Rammler relationship can be expressed in terms of the cumulative mass distribution as:

No.	Density of sediment grains ρ_s (kg/m^3)	D_5 (μm)	D_{50} (μm)	D_{95} (μm)	n	R^2
Type 1	2503	22.4	113.52	678.28	2.85	0.997
Type 2	2345	25.25	112.95	516.79	1.40	0.996
Type 3	2025	10.68	37.18	86.05	2.14	0.999

Table 2: Several basic properties of sands with three different types.

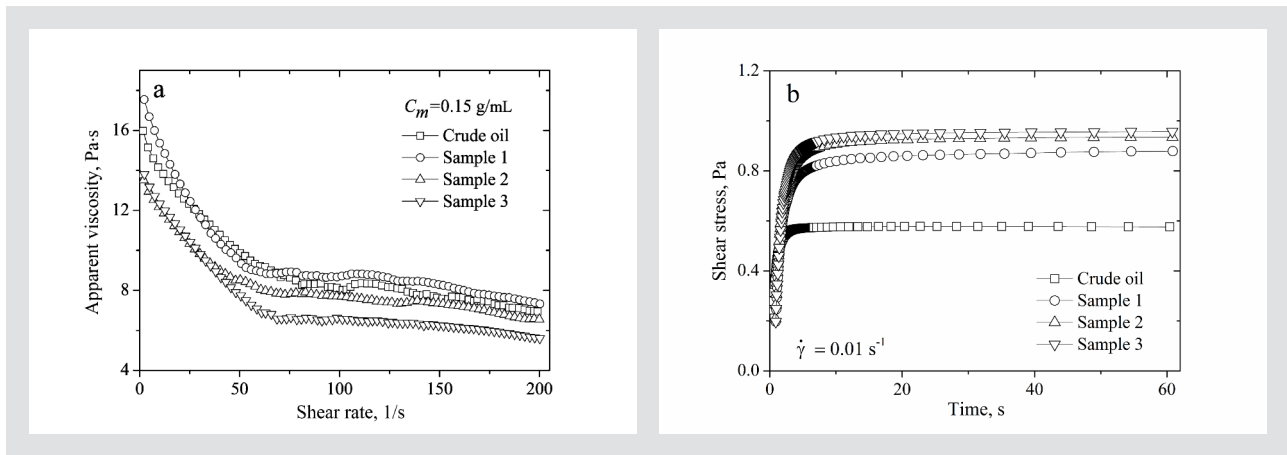


Figure 2: Rheograms of heavy crude oil containing sands for three different samples at 30 °C.

$$F_m(d) = 1 - \exp\left(-\frac{d}{\delta}\right)^n \quad (1)$$

In this equation, δ and n are two empirical constants. The parameter δ can be obtained using n and the mass median diameter D_{50} in the following equation:

$$\delta = \frac{D_{50}}{0.693^{1/n}} \quad (2)$$

Figure 1 further demonstrates that the regression correlation coefficient R^2 is larger than 0.99. Therefore, it is appropriate to use the Rosin-Rammler distribution function to describe sand size distributions.

2.2 EXPERIMENTS

Rheological measurements were conducted using the Haake RS6000 rheometer equipped with a coaxial cylinder sensor system (Z38 DIN, with a gap width of 2.5 mm and a sample volume of 30.8 cm³) and a four-bladed vane type rotor FL40 (with a diameter of 40 mm and a gap width of 1.5 mm). This equipment features a liquid temperature-controlled system that allows the sensor system to reach a fixed temperature and maintain this temperature throughout the experiment. Furthermore, when choosing a rheometer with a coaxial cylinder sensor to analyze suspensions, it is necessary to achieve a ratio of particle size to gap size of less than 1/3 to avoid the disturbing issues [20]. According to this criterion, the maximum particle size in the present study should be less than 0.83 mm. In practice, only 3.55 % of sample 1 particle diameters and 1.46 % of sample 2 particle diameters exceed this 0.83 mm limit. The maximum particle diameter in sample 3 is 0.74 mm and thus does not exceed the 0.83 mm maximum. Consequently, it is assumed that the low proportions of large particle sizes in these samples produce only minimal interference and that these results are acceptable.

In this study, samples were prepared in batches of 300 mL and pre-heated to a fixed temperature. Homog-

enization of heavy crude oil and sand was then achieved using a three-blade stirrer at a fixed low speed. After homogenization, rheological properties of the samples were characterized and measured using a rheometer. To ensure analytical quality, the preparation processes of different samples remained independent of each other, and all measurements were performed three times to obtain good repeatability. In the thixotropy measurement, the hysteresis loop was obtained by increasing the shear rate from 0 to 200 s⁻¹ over a period of 200 s and then decreasing the shear rate from 200 s⁻¹ to 0 at a fixed temperature. At the same time, to study the samples' rheological properties at a temperature of 20 °C, shear stress was increased from 0 to 1600 Pa and then reduced back to 0 Pa. During this oscillatory measurement, an amplitude sweep was performed prior to the subsequent frequency sweep to constrain the selected stress sweep within a linear viscoelastic region. Stress sweeps were conducted at a fixed frequency of 5 Hz in the range of 0.001 ~ 200 Pa, and frequency sweeps were carried out at a fixed shear stress of 1 Pa. Experimental data were also obtained by recording the elastic modulus G' , loss modulus G'' , and complex viscosity η^* .

3 RESULTS AND DISCUSSION

3.1 APPARENT VISCOSITY

Figure 2 depicts rheograms of samples with different size distributions at a constant mass concentration of 0.15 g/mL. The figure demonstrates that after heavy crude oil is blended with sand, all samples show strong shear-thinning behavior. Apparent viscosity also increases with particle size at a fixed concentration. For example, at a given mass concentration of 0.15 g/mL, heavy crude oil containing sand yields a lower apparent viscosity than pure crude oil. This maybe because heavy crude oil becomes more shear-thinning with the addition of small particle sizes, thus reducing its apparent viscosity. However, increasing particle size could also enhance the interfacial interaction between these par-

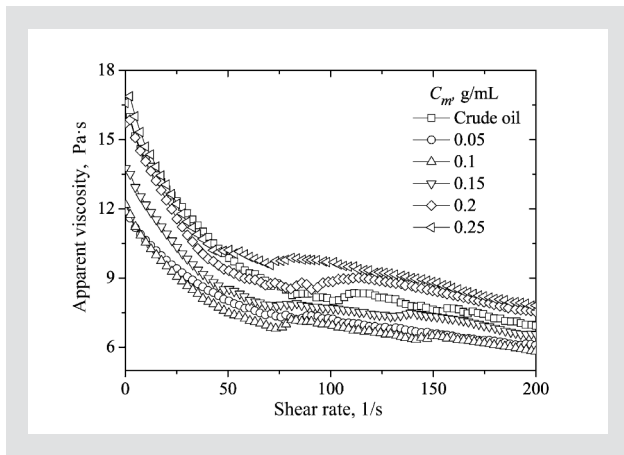


Figure 3: Rheogram of sample 2 with different sand mass concentrations at 30 °C.

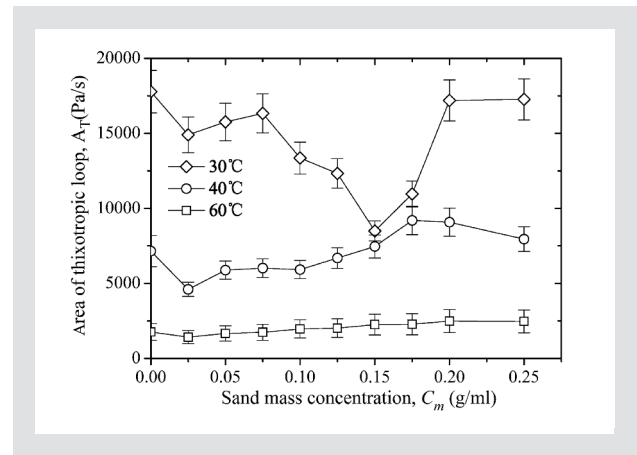


Figure 5: Effects of sand mass concentration on the area of the thixotropic loop at three different system temperatures.

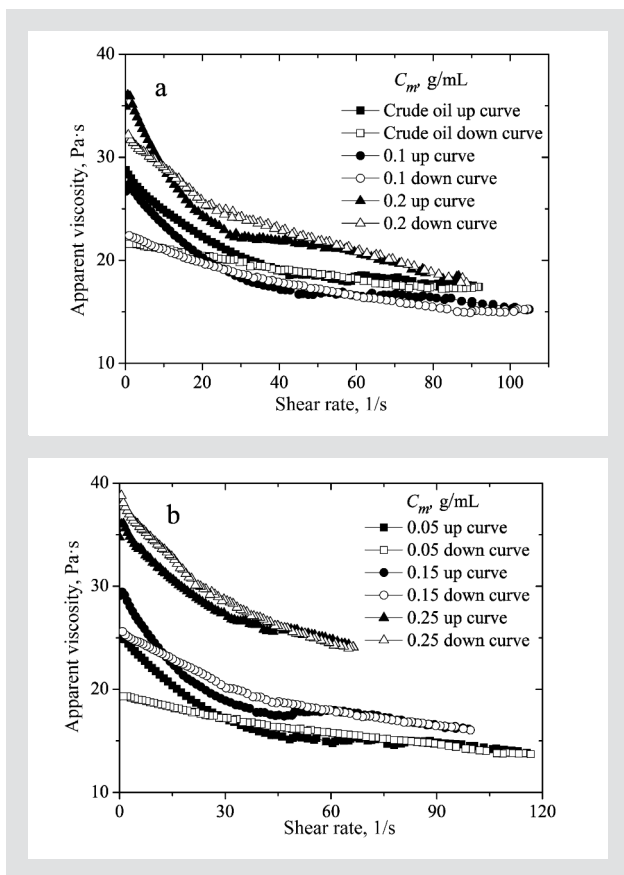


Figure 4: Flow curves of sample 2 obtained using the hysteresis technique across a range of different mass concentrations at 20 °C.

ticles, thus increasing its apparent viscosity. Figure 3 depicts rheograms of sample 2 across a range of different mass concentrations at 30 °C: When the mass concentration is larger than 0.2 g/ml, the apparent viscosity of heavy crude oil containing sand is higher than that of pure crude oil. At low mass concentrations, heavy crude oil blended with sand becomes more shear-thinning. However, the interfacial interactions between particles could be enhanced with further increases in sand mass concentration. Therefore, these data suggest that

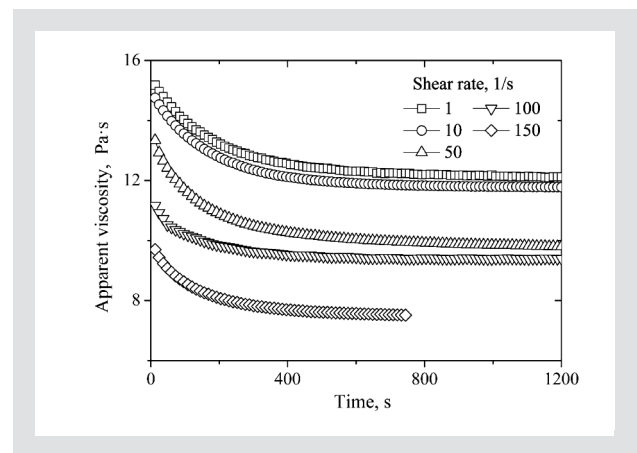


Figure 6: Results of time-dependent analyses of heavy crude oil at different shear rates at 30 °C.

trends in apparent viscosity are influenced by two different types of interactions.

3.2 THIXOTROPIC BEHAVIOR

The thixotropic behavior of heavy crude oil plays an important role in influencing the design of pipe network systems and the restart operations of flow. There are various methods of measuring thixotropic behavior, including the hysteresis technique [21], the stepwise changes method [22], and the start-up experiment [23]. In the present study, the thixotropic behavior of samples was measured using the hysteresis technique. Figure 4 depicts the flow curves of sample 2 for a range of different mass concentrations at 20 °C. Closed symbols represent a run with an increasing shear rate, and the open symbols represent a run with a decreasing shear rate. The up and down curves vary significantly: for example, as the mass concentration increases, the down curves are higher than the up curves. This may be explained by the fact that the internal structure of heavy crude oil containing sands changes greatly as the mass concentration increases. Furthermore, Figure 5 depicts the effects of sand mass concentration on the area of

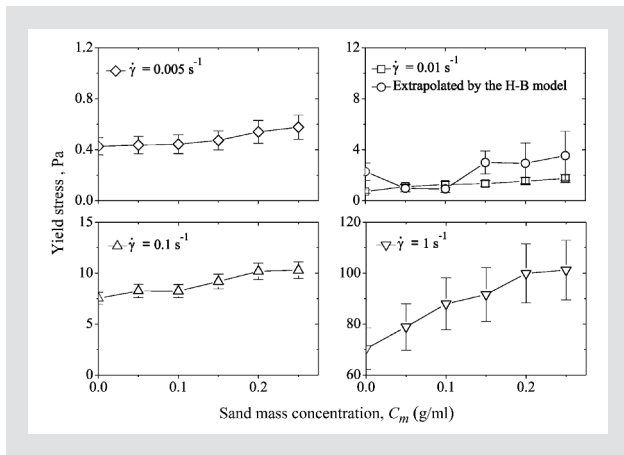


Figure 7: Effect of vane rotational speed on yield stress for sample 2 at various sand mass concentrations.

the thixotropic loop at three different system temperatures. At low mass concentrations, the area of thixotropic loop decreases as the mass concentration increases, before reaching a minimum value. After this point, the area of the thixotropic loop increases steadily with further increases in mass concentration. The area of the thixotropic loop also decreases significantly with increasing temperature. Figure 6 depicts time-dependent measurements of heavy crude oil at different shear rates. These results were obtained when the shear rate was changed from 0.1 s^{-1} to 10 s^{-1} . In these experiments, viscosity first decreases before reaching a relatively steady state, similar to the results of the steady shear measurements shown in Figure 2. A comparison between the viscosities obtained by transient viscosity measurements and those obtained by steady viscosity measurements is shown in Table 3. These data demonstrate that as the shear rate increases, the difference between the two measurements decreases. In other words, the steady measurements eventually reach a steady state [24].

3.3 YIELD BEHAVIOR

Yield stress is generally defined as the stress at which a material transitions from behaving as either elastic (i.e. solid-like) or viscous (i.e. liquid-like). Therefore, defining the yield stress of heavy crude oil is important for designing the flow loop system. In this work, yield stresses were measured using the vane method, which has become the standard method of measuring yield

Shear rate (s^{-1})	Viscosity by the transient shear tests (Pa·s)	Viscosity by the steady shear tests (Pa·s)	Relative Deviation, %
1	12.12	15.97	13.7
10	11.78	14.06	8.82
50	10.11	9.87	1.20
100	8.15	8.39	1.45
150	7.51	7.59	0.53

Table 3: Comparison of viscosity values measured by transient rheological measurements and steady rheological measurements.

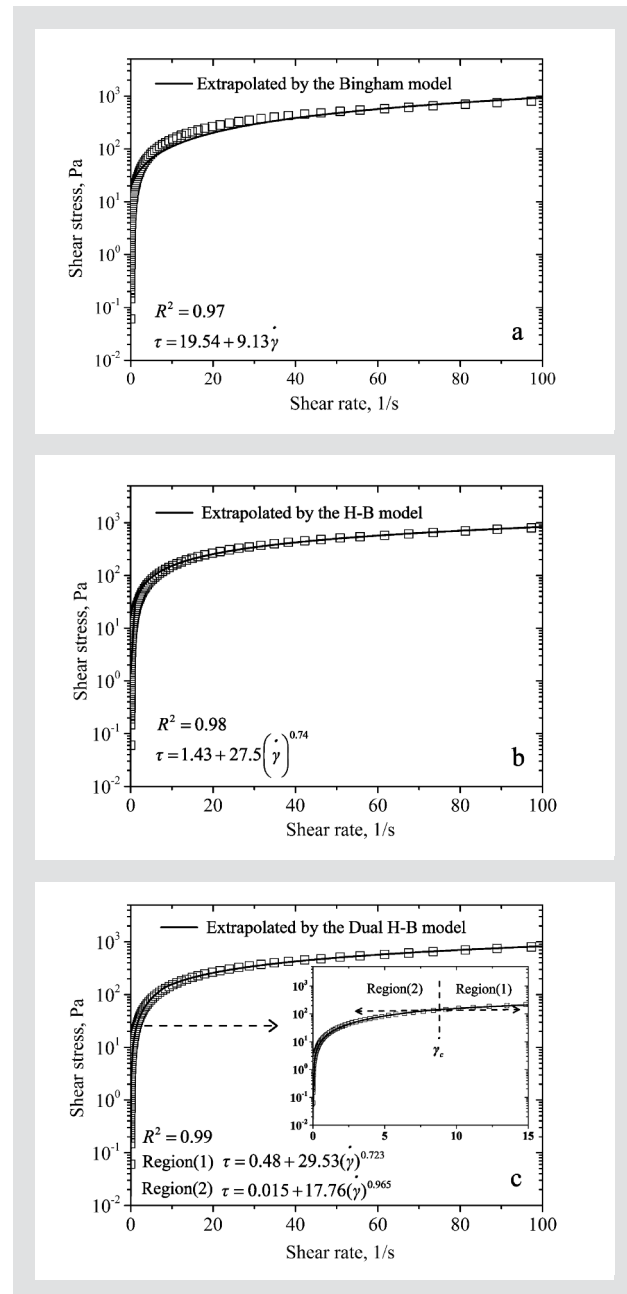


Figure 8: Comparison of experimental data with flow curves predicted by the Bingham model, the Herschel-Bulkley model, and the Dual-Herschel-Bulkley model for heavy crude oil at $30 \text{ }^\circ\text{C}$.

stress due to its simplicity and ability to prevent slip during shearing. In addition to the vane method, yield stresses were also obtained by extrapolating flow curves to a zero shear rate [16]. To obtain reliable data using the vane test, it is essential to study the effect of vane rotational speed on yield stress. Nguyen and Boger [25] analyzed the effect of rotational speed on the yield stress of red mud suspensions: Results demonstrated that yield stress is almost independent of the shear rate over a range of $0.002 - 0.13 \text{ s}^{-1}$. They proposed that satisfactory yield stress measurements should, therefore, be obtained at a sufficiently low rotational speed because viscous resistance effects can occur at high rotational speeds. Additionally, Gutierrez and Pawlik [16] investigated the effect of vane rotational speed on yield

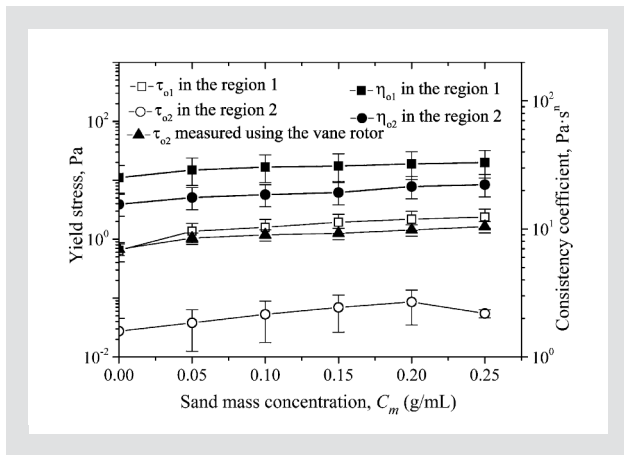


Figure 9: Yield stress and consistency coefficient as a function of sand mass concentration as determined by flow curve extrapolation for sample 2.

stress in slurries of prepared ore samples. Their results demonstrated that torque values remain relatively constant at rotational speeds lower than 1 rpm and that their obtained shear stress, which corresponds on a flow curve to a shear rate of approximately 0.01 s^{-1} , was very close to their actual yield stress. Maciel et al. [26] also observed the same phenomenon. Based on these previously published results, tests were conducted to gauge the effects of shear rate on yield stress prior to conducting the vane test.

Figure 7 depicts the effects of shear rate on yield stress at different mass concentrations. Values of yield stress are relatively stable with increasing mass concentrations when the shear rate is lower than 0.1 s^{-1} . However, when the shear rate reaches 1.0 s^{-1} , the yield stress begins to rapidly increase. Comparing the yield stresses predicted by the Herschel-Bulkley model with those obtained by the vane test demonstrates that the measured and predicted results are similar at a shear rate of 0.01 s^{-1} . Therefore, based on these experimental observations, all vane tests undertaken to measure yield stress in this work were conducted at a shear rate of 0.01 s^{-1} . Moreover, it is apparent that yield stress increases with increasing shear rates and decreases with increasing sediment particle size, as is shown in Figure 2b. An optimal method of predicting the flow behavior of suspensions is to exploit a theoretical model to fit the experimental data and thereby obtain the yield stress. The simplest theoretical model used to de-

termine the yield stress of fluids is the Bingham model, which exhibits a linear stress-strain relationship when shear stress is in excess of yield stress. However, in most cases, it is not possible to fit experimental data with satisfactory accuracy in this model over a low range of shear rates [27]. To overcome this problem, Xu and Huhe [28] developed the Dual-Herschel-Bulkley model to predict yield stress. The Dual-Herschel-Bingham model can be described using six parameters based on two different regions of shear rates:

$$\begin{aligned} \tau &= \tau_{o1} + \eta_{o1}(\dot{\gamma})^{n_1} & \dot{\gamma} > \dot{\gamma}_c \\ \tau &= \tau_{o2} + \eta_{o2}(\dot{\gamma})^{n_2} & \dot{\gamma} \leq \dot{\gamma}_c \end{aligned} \quad (3)$$

In this equation, τ_o represents the yield stress in Pa, η_o and n represent the fluid consistency coefficient in $\text{Pa}\cdot\text{s}^n$ (defined as the apparent viscosity of the Herschel-Bulkley model), and the flow behavior index. Subscripts 1 and 2 refer to region 1 and region 2, respectively. $\dot{\gamma}_c$ represents the critical shear rate and can be solved numerically using the following equation:

$$\frac{\eta_{o2}(\dot{\gamma}_c)^{n_2} - \eta_{o1}(\dot{\gamma}_c)^{n_1}}{\tau_{o1} - \tau_{o2}} - 1 = 0 \quad (4)$$

In this equation, τ_{o1} , τ_{o2} , η_{o1} , η_{o2} , n_1 and n_2 are assumed to be known quantities. Therefore, an iteration procedure is needed to obtain the critical shear rate. When $n_1 = n_2 = 1$, Equation 3 can represent a simplified 'first guess' of this iteration procedure. The six parameters extrapolated by the Dual-Herschel-Bulkley model are listed in Table 4. Figure 8 presents a comparison of experimental data with the flow curves predicted by the Bingham, Herschel-Bulkley, and Dual-Herschel-Bulkley models. As the figure demonstrates, the Dual-Herschel-Bulkley model yields better predicted results than the other two models. Figure 9 displays the yield stress and consistency coefficient obtained using the flow curve extrapolation as a function of sand mass concentration. This figure demonstrates that measured yield stresses are close to those extrapolated in region 1 with higher values of yield stress. These findings further prove the validity of this model. Furthermore, these data indicate that yield stress and the consistency coefficient increase with increasing sediment mass concentration.

3.3 VISCOELASTIC PROPERTIES

Figures 10 and 11 display variations in the elastic modulus and the loss modulus as a function of shear stress

Mass concentration	Region (1)				Region (2)			
	τ_{o1} (Pa)	η_{o1} ($\text{Pa}\cdot\text{s}^n$)	n_1	R_1^2	τ_{o2} (Pa)	η_{o2} ($\text{Pa}\cdot\text{s}^n$)	n_2	R_2^2
0	0.48	29.528	0.723	0.997	0.015	17.761	0.965	0.999
0.05	1.015	33.843	0.687	0.999	0.02	20.079	0.951	0.998
0.1	1.191	35.691	0.673	0.999	0.028	21.131	0.95	0.999
0.15	1.451	36.4	0.703	0.999	0.039	21.945	0.953	0.998
0.2	1.63	37.79	0.725	0.999	0.05	24.447	0.953	0.999
0.25	1.784	38.693	0.742	0.999	0.061	25.276	0.947	0.999

Table 4: Parameters extrapolated by the Dual-Herschel-Bulkley model for sample 2.

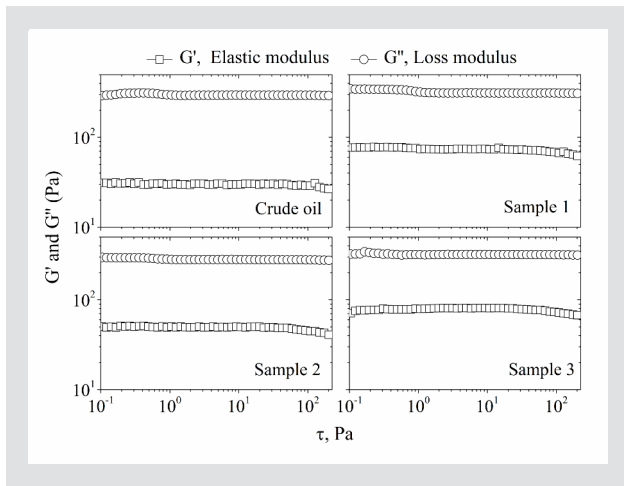


Figure 10: Variation of the elastic modulus and the loss modulus as a function of shear stress for three different samples at a fixed mass concentration ($C_m = 0.15$ g/ml).

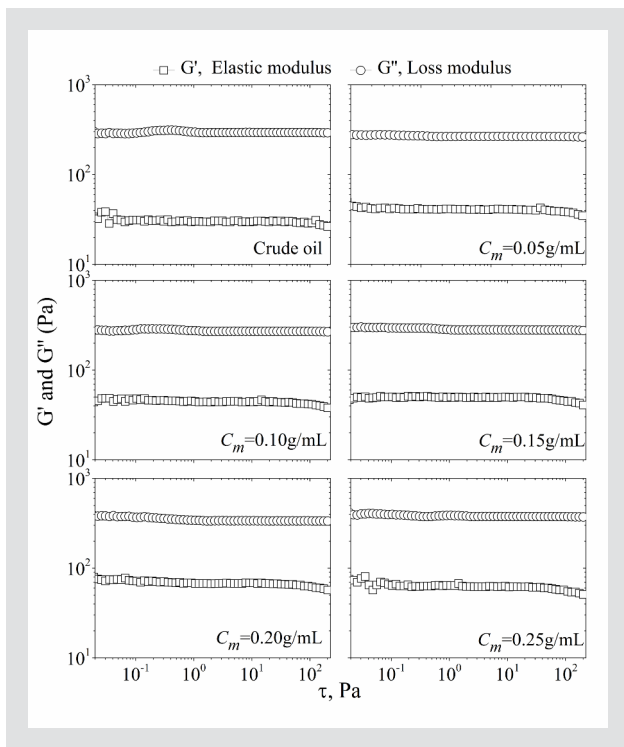


Figure 11: Variation of the elastic modulus and the loss modulus of sample 2 as a function of shear stress at a fixed frequency ($f = 5$ Hz).

with a fixed shear stress sweep frequency ($f = 5$ Hz). These measurements were undertaken to obtain these parameters to recognize the linear region. These figures demonstrate that the shear stress dependence on the elastic and loss modulus is rather weak. In contrast, the linearity of viscoelastic behavior in the sample is very good over a wide range of stress amplitudes from 0.1–100 Pa. Therefore, $\tau = 1$ Pa was selected for the following frequency sweep. The results of the frequency sweep conducted at a fixed shear stress are depicted in Figures 12 and 13. These figures demonstrate that the loss modulus is greater than the elastic modulus over

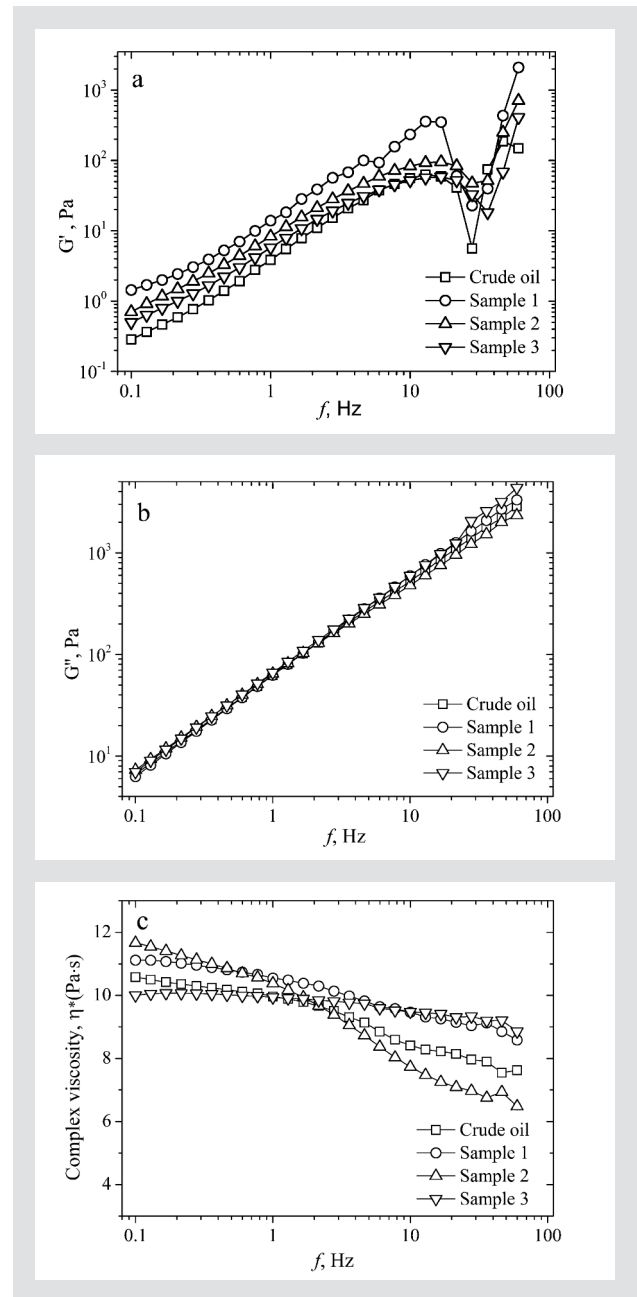


Figure 12: Variations in the elastic modulus, loss modulus and complex viscosity as a function of frequency at a fixed shear stress ($\tau = 1$ Pa) in various samples

the entire range of frequency, indicating that heavy crude oil containing sand is predominantly viscous. The elastic modulus can be enhanced when sand is added into heavy crude oil, but it does not increase significantly when the mass concentration is increased. These figures further demonstrate that the elastic modulus increases with increasing particle size. When the frequency reaches approximately 30 Hz, the elastic modulus sharply decreases. This may be because the structure of the sample changes greatly under high-frequency conditions. Furthermore, the loss modulus increases almost linearly with increasing frequency. Figures 12c and 13c display changes in complex viscosity with frequency. The decrease in complex viscosity becomes more significant with changes in sand mass concentration. For

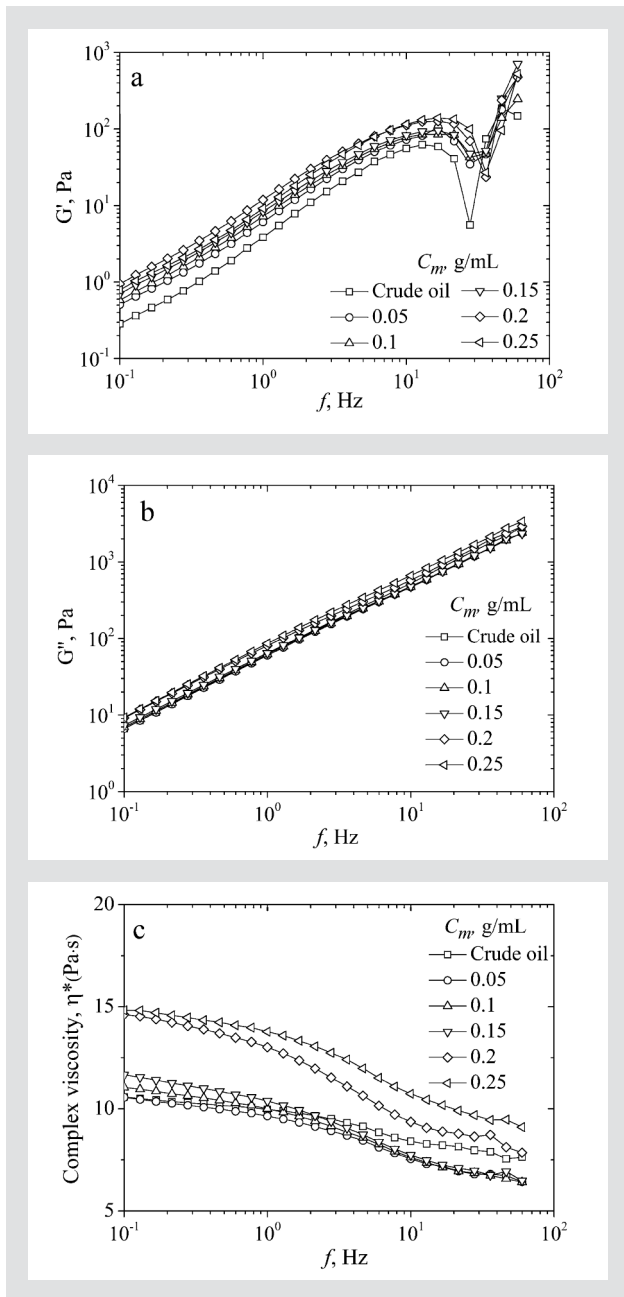


Figure 13: Variations in the elastic modulus, loss modulus and complex viscosity as a function of frequency at a fixed shear stress ($\tau = 1 \text{ Pa}$) for sample 2 at various sand mass concentrations).

example, in the region of low frequency sweep, complex viscosity increases with increasing sediment size. Additionally, the effects of sand mass concentration on complex viscosity are similar to the observed effects on apparent viscosity. When comparing these data to those presented in Figures 2 and 3, it is clear that at a fixed concentration, the value of complex viscosity is slightly less than that of apparent viscosity. In effect, the hydrocyclones used to de-sand crude oil typically operate at a high tangential acceleration and thus have large angular velocities. Figure 14 thus displays observed variations in complex viscosity, the elastic modulus, and the loss modulus with sand mass concentration at angular velocities of $\omega = 6.28$ and 62.8 rad/s . It is im-

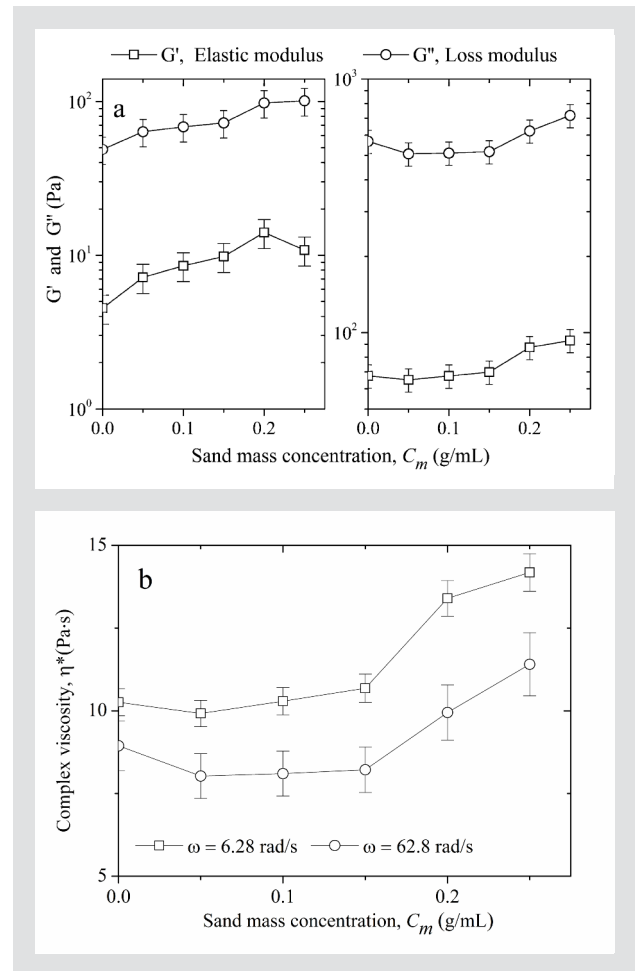


Figure 14: Variations of complex viscosity, the elastic modulus and the loss modulus with sand mass concentration at angular velocities of $\omega = 6.28$ and 62.8 rad/s .

portant to note that as sand mass concentration increases, the elastic modulus, the loss modulus and the complex viscosity all also increase. Furthermore, it is clear that the effects of angular velocity are greater on the elastic modulus and the loss modulus than they are on complex viscosity.

4 CONCLUSIONS

This work represents a study on the rheological properties of heavy crude oil containing sand. The effects of sand size distribution and mass concentration on apparent viscosity, thixotropic behavior, yield stress and viscoelastic properties were investigated. Heavy crude oil containing sand shows a strong shear-thinning behavior and a certain degree of thixotropic behavior. When heavy crude oil is blended with a small amount of sand, the apparent viscosity of the mixture decreases. However, as the sand mass concentration increases, the apparent viscosity will increase until it exceeds that of the heavy crude oil. Similarly, the area of the thixotropic loop quickly decreases before reaching a minimum value and then increases steadily. Yield stress and the fluid consistency coefficient increase with increas-

ing sediment mass concentration. Apparent viscosity also increases with increasing particle size at a fixed concentration, whereas, in contrast, yield stress gradually decreases. In general, adding sand and increasing the sediment size of heavy crude oil increases its elastic modulus, loss modulus and complex viscosity. Additionally, its complex viscosity becomes slightly less than its apparent viscosity. These results provide insights that are ultimately useful for the process of removing sand from heavy crude oil.

ACKNOWLEDGEMENTS

The authors gratefully acknowledge that the work described here is financially supported by the Strategic Priority Research Program of the Chinese Academy of Science (Grant No: XDB22030101).

REFERENCES

- [1] Dusseault MB: Comparing Venezuelan and Canadian heavy oil and tar sands, The Petroleum Society's Canadian International Petroleum Conference, Calgary (2001) June 12–14.
- [2] Ghannam MT, Hasan SW, Abu-Jdayi B, Esmail N: Rheological properties of heavy & light crude oil mixtures for improving flowability, J. Pet. Sci. Eng. 81 (2012) 122–128.
- [3] Martinez-Palou R, Mosqueira MDL, Zapata-Rendon B, Mar-Juarez E, Bernal-Huicochea C, Clavel-Lopez JC, Aburto J: Transportation of heavy and extra-heavy crude oil by pipeline: A review, J. Pet. Sci. Eng. 75 (2011) 274–282.
- [4] Ashrafizadeh SN, Kamran M: Emulsification of heavy crude oil in water for pipeline transportation, J. Petro. Sci. Eng. 71 (2010) 205–211.
- [5] Chen XP, Xu JY, Zhang J: A Simple model for predicting the two-phase heavy crude oil horizontal flow with low gas fraction, Chem. Eng. Commun. 203 (2016) 1131–1138.
- [6] Naiya TK, Banerjee S, Kumar R, Mandal A: Heavy crude oil rheology improvement using naturally extracted surfactant, SPE Oil & Gas India Conference and Exhibition, Mumbai (2015) November 24–26.
- [7] Liddell PV, Boger DV: Yield stress measurements with the vane, J. Non-Newtonian Fluid Mech. 63 (1996) 235–261.
- [8] Gutierrez L, Pawlik M: Observations on the yielding behavior of oil sand slurries under vane and slump tests, Can. J. Chem. Eng. 93 (2015) 1392–1402.
- [9] Soares EJ, Thompson RL, Machado A: Measuring the yielding of waxy crude oils considering its time-dependency and apparent-yield-stress nature, Appl. Rheol. 23 (2013) 62798.
- [10] Mortazavi-Manesh S, Shaw JM: Thixotropic rheological behavior of Maya crude oil, Energy Fuels 28 (2014) 972–979.
- [11] Abivin P, Taylor SD, Freed D: Thermal behavior and viscoelasticity of heavy oils, Energy Fuels 26 (2012) 3448–3461.
- [12] Wardhaugh LT, Boger DV, Tonner SP: Rheology of waxy crude oils, SPE International Meeting on Petroleum Engineering, Tianjin (1988) November 1–4.
- [13] Konijn BJ, Sanderink OBJ, Kruyt NP: Experimental study of the viscosity of suspensions: effect of solid fraction, particle size and suspending liquid, Powder Technol. 266 (2014) 61–69.
- [14] Dai Q, Chung KH: Bitumen-sand interaction in oil sand processing, Fuel 74 (1995) 1858–1864.
- [15] Hasan MDA, Fulem M, Bazyleva A, Shaw JM: Rheological properties of nanofiltered Athabasca bitumen and Maya crude oil, Energy Fuels 23 (2009) 5012–5021.
- [16] Gutierrez L, Pawlik M: Observations on the yielding behavior of oil sand slurries under vane and slump tests, Can. J. Chem. Eng. 93 (2015) 1392–1402.
- [17] Koenigsberg W, Selverian JH: Zone method for representing relaxation characteristics of viscoelastic materials, Appl. Rheol. 15 (2005) 160–171.
- [18] Jamaluddin AKM, Bowen CT, Gillies R, Small M, Nazarko TW: Characteristics of heavy-oil-in-water emulsions containing produced sand, Can. J. Chem. Eng. 72 (1994) 380–384.
- [19] Yaghi B: Rheology of oil-in-water emulsions containing fine particles, J. Pet. Sci. Eng. 40 (2003) 103–110.
- [20] Schramm G: A practical approach to rheology and rheometry, Gebrüder Haake, Karlsruhe, Germany (1994).
- [21] Yoon C, Heister SD, Campanella OH: Modeling gelled fluid flow with thixotropy and rheological hysteresis effects, Fuel 128 (2014) 467–475.
- [22] Labanda J, Llorens J: A structural model for thixotropy of colloidal dispersions, Rheol. Acta. 45 (2005), 305–314.
- [23] Mewis J, Wagner NJ: Thixotropy, Adv. Colloid. Interfac. 147-148 (2009) 214–227.
- [24] Ardakani HA, Mitsoulis E, Hatzikiriakos SG: Capillary flow of milk chocolate, J. Non-Newtonian Fluid Mech. 210 (2014) 56–65.
- [25] Nguyen QD, Boger DV: Yield stress measurement for concentrated suspensions, J. Rheol. 27 (1983) 321–349.
- [26] Maciel GF, Santos HK, Ferreira FO: Rheological analysis of water clay compositions in order to investigate mudflows developing in canals, J. Brazil. Soc. Mech. Sci. Eng. 31 (2009) 64–74.
- [27] Coussot P, Proust S, Ancey C: Rheology interpretation of deposits of yield stress fluids, J. Non-Newtonian Fluid Mech. 66 (1996) 55–70.
- [28] Xu J, Huhe A: Rheological study of mudflows at lianyungang in China, Inter. J. Sediment Res. 31(2016) 71–78.

